

Partial densities of states for silver bromide and silver iodobromide

M. G. Mason and Y. T. Tan

Research Laboratories, Eastman Kodak Company, Rochester, New York 14650

T. J. Miller and G. N. Kwawer*

Department of Physics, University of Illinois at Urbana-Champaign, 1110 West Green Street, Urbana, Illinois 61801

F. C. Brown

Department of Physics (FM-15), University of Washington, Seattle, Washington 98195

A. B. Kunz

Department of Physics, Michigan Technological University, Houghton, Michigan 49931

(Received 12 March 1990)

The valence-band photoemission of silver bromide and silver iodobromide has been measured with use of synchrotron radiation in the region of the Ag $4d$ Cooper minimum. The large change in ionization cross section in this region permits the determination of the individual halogen p and silver $4d$ partial densities of states (PDOS). The energy-distribution curves (EDC's) were recorded at liquid-nitrogen temperatures to prevent photolysis and take advantage of the significant line narrowing which occurs in the silver halides at low temperatures. The results are in good agreement with experiments using rare-gas resonance lines and with previously calculated energy-band structures. Changes in the halogen PDOS with the addition of iodide indicate that the narrowing of the band gap is due to the broadening of the uppermost antibonding halogen bands. The PDOS were calculated for pure AgBr using a nonrelativistic, self-consistent, Hartree-Fock theory and show good agreement with the experimental results.

I. INTRODUCTION

In the alkali halides the most loosely bound electrons on the halogen and the alkali-metal ions are well separated in energy.¹⁻³ This leads to a relatively simple valence band composed almost exclusively of halogen p -like orbitals. In the noble-metal halides the situation is significantly complicated by the presence of the metal d orbitals which are in near degeneracy with those of the halogen.⁴⁻¹⁸ This near degeneracy leads to strong hybridization and considerable complexity in the valence-band structure. For example, in the rock-salt-structure materials, AgCl and AgBr, this orbital mixing has profound effects, causing these materials to have indirect band gaps and large valence-band widths. In the context of photoemission spectra, this mixing means that valence-band energy-distribution curves (EDC's) will be a composite of both the halogen and metal partial densities of states (PDOS's). The relative proportions will vary according to the energy-dependent ionization cross sections. In an ideal case, for each type of orbital composing the valence band there would exist a photon energy or energy range where its contribution to the experimental spectrum would dominate. By recording spectra at each of these energies, all of the constituent partial densities of states could be directly measured. This ideal situation is closely approximated in the Cu-Au alloys.¹⁹ At low photon energies the EDC's reflect mainly the Au $5d$ density of states, but near the Au $5d$ Cooper minimum, at about 160 eV, the EDC's are due primarily to the Cu $4d$ density

of states. As pointed out by Wertheim,¹⁹ this procedure should have wide applicability for compounds or alloys containing $4d$ - or $5d$ -group elements.

In the silver halides the procedure for determining partial densities of states is somewhat more complex than in the copper-gold alloys. Whereas the valence Ag $4d$ orbitals do show a significant Copper minimum at around 130 eV,²⁰⁻²³ the halogen ionization cross sections are not large enough to produce a spectrum characteristic of the pure halogen density of states.²⁴ It is, however, still possible to extract the partial densities of states from measured EDC's. It is only necessary that the ionization cross sections be known and that the relative values change significantly with photon energy. This procedure was pioneered by Cardona and co-workers and has been applied to the silver^{9,10} and cuprous halides,⁹ as well as the ternary compounds AgInTe₂ and CuInS₂.²⁵ More recently, the partial density of states in Cu₇₅Pd₂₅ has been determined with this method from synchrotron-radiation studies.²⁶ The basic assumption is that the experimental intensity, $N(E, h\nu)$, where E is the electron kinetic energy and $h\nu$ is the photon energy, is related to the ionization cross section per electron, $\sigma_i(h\nu)$, and the partial density of states, $\rho_i(E)$, by the simple relationship

$$N(E, h\nu) = C(E, h\nu) [\rho_p(E)\sigma_p(h\nu) + \rho_d(E)\sigma_d(h\nu)] . \quad (1)$$

The proportionality constant, $C(E, h\nu)$, contains experimental variables such as photon flux and analyzer transmission function as well as effects due to the electron

escape depth. The justification for this simple model and the approximations inherent in it have been discussed in detail in the earlier work cited above.^{9,10,26}

At the photon energies used in the present study, the kinetic energy changes little over the width of the valence band, so the proportionality constant in Eq. (1) is practically independent of E . This allows the equation to be solved for the partial densities of states, with $C(E, h\nu) = C(h\nu)$ being determined from the requirement that the sum of the partial densities of states over all energies is simply the total number of valence electrons of a given type:

$$\int \rho_p dE = 6 \quad (2)$$

and

$$\int \rho_d dE = 10, \quad (3)$$

and the fact that the area under the EDC is simply the integral of Eq. (1), given by

$$\mathcal{A} = \int N(E, h\nu) = C(h\nu) [10\sigma_d(h\nu) + 6\sigma_p(h\nu)]. \quad (4)$$

With $C(h\nu)$ thus determined, the experimental data $N(E, h\nu)$, Eq. (1), has only two unknowns, the halogen p and silver d partial densities of states. If EDC's are then measured at two photon energies, their intensities at every binding energy, $N(E, h\nu)$, will give two linearly independent equations which can be solved for the p and d partial densities of states.^{9,10} Their properly normalized sum will then give an experimentally determined, total density of states, $\rho(E)$. This procedure is almost identical to that used by Tejada *et al.*^{9,10,25} It works well for systems where surface core-level shifts are small enough to be disregarded.¹⁹ This study extends such work to the iodobromides utilizing samples and an experimental geometry that prevent angular distortions. Furthermore, EDC's were recorded only at low temperature where linewidths are significantly narrowed²⁷⁻²⁹ and photolysis almost completely quenched.³⁰

We have also used synchrotron radiation, which allows us to select those photon energies where the determination of the partial densities of states can best be realized. The earlier work on the silver halides¹⁰ relied on rare-gas discharge sources for photoexcitation; specifically, He I (21.2 eV) and He II (40.8 eV) radiation. In principle, the large variation in halogen cross section expected in this range should allow for an excellent determination of partial densities of states. Unfortunately, the halide cross sections were not known experimentally and were taken from "semiquantitative comparisons" with those of the isoelectronic rare gases.³¹ This is certainly a reasonable first approximation but could be in considerable error. Calculations and recent experimental results on chlorine as well as the rare gases show that the cross sections change very rapidly in this photon-energy range.^{24,32-34} Even today, the absence of experimental cross-section data remains a serious limitation in determining accurate densities of states. The experimental photoionization cross sections of both atomic and molecular chlorine are now available,³⁴ but that of bromine is not.

Because of the lack of a complete set of experimental

values, we have chosen to use theoretical cross sections²⁴ in determining the PDOS. Some of the errors that are most likely to occur with this approach can be minimized by using synchrotron radiation. We are able to record EDC's at photon energies on either side of the Cooper minimum and avoid regions of high cross-section variation. At these energies the calculations are less sensitive to details of the wave function and should be more reliable. These and other questions posed by uncertainties in ionization cross sections will be looked at in detail in Sec. III where the experimental PDOS are actually derived and compared with the p - and d -projected density of states from band theory.

II. EXPERIMENTAL DETAILS

In order for experimental EDC's to reflect densities of states as presented in Eq. (1), it is necessary that care be taken to avoid certain angular effects, which can be very significant in photoemission from solid materials. Recently the rather large effects from atomiclike angular anisotropies in these materials have been studied in considerable detail.^{22,23} These can most easily be avoided by recording EDC's at the so-called "magic angle," where the analyzer is placed at an angle of 54.7° from the polarization vector of the incoming photon beam. In this configuration, spectral intensity is determined by the total angular integrated cross sections σ , rather than by the differential cross sections $d\sigma/d\Omega$. All spectra were recorded in this experimental geometry with the analyzer in the horizontal plane. EDC's recorded with the analyzer and polarization vector collinear showed significant differences, indicating that this factor must be considered if measured intensities are to be determined by the total, integrated cross sections. A typical hemispherical analyzer has acceptance angles on the order of 6°, which does not give sufficient angle averaging to overcome this effect. The second major concern for angular distortion of the spectra arises from direct transition effects.³⁵ In crystalline materials, particularly at low photon energy and low temperature, valence-band excitations tend to conserve crystal momentum and produce a very anisotropic distribution of emitted electrons. This is overcome by making the sample highly disordered so that these spatial anisotropies are averaged out and the intensity is again determined only by the total angle-independent cross section.

Samples were prepared in an ultrahigh-vacuum (UHV) evaporation chamber that could be isolated from the main analysis chamber. 1-cm glass microscope slides, overcoated with a thick layer of gold to ensure electrical conductivity, were placed in the chamber, and pumped to the high- 10^{-9} - or low- 10^{-8} -Torr range. About 10 000 Å of silver was evaporated onto the gold-coated surface. The sample was then transferred to the main analysis chamber, which maintained a base pressure of about 2×10^{-10} Torr and was sputtered with argon (4×10^{-5} Torr, 0.5 keV, 35 mA) for 40 min. This procedure served to further randomize the polycrystalline silver and produced clean core-level and valence-band photoemission spectra. The sample was then transferred

back to the evaporation chamber, where the silver halide was slowly vapor-deposited, in the dark, from a resistively heated platinum filament.³⁶ A total of about 400 Å was normally evaporated to form a continuous layer, which was yet thin enough to prevent charging in these excellent low-temperature insulators. The $\text{AgBr}_{1-x}\text{I}_x$ was prepared by a very slow evaporation of the material onto an existing of AgBr sample and then annealed at 200°C. This was done because, even with low concentrations of iodide and low evaporation temperature, a very iodide rich film is favored.³⁷ By evaporating the $\text{AgBr}_{1-x}\text{I}_x$ onto pure AgBr and annealing, we are able to lower the iodide concentration, which was experimentally determined from the I 4*d* and Br 3*d* core-level intensities to be about 12% iodide. The sample was then transferred back into the analysis chamber and mounted on a liquid-nitrogen-cooled precision manipulator.

All viewports were covered by yellow filters to prevent exposure to actinic radiation, and there was no exposure to synchrotron radiation until the sample had cooled to liquid-nitrogen temperature. At these temperatures the core and valence-band spectra are significantly narrowed^{17,18,27,28} and photolysis is almost entirely quenched.³⁰ The absence of low-temperature photolysis was confirmed by monitoring the core-level intensities of Ag, Br, and I throughout the experiments. At low temperature the intensities were independent of exposure, while at room temperature a 30% loss in Br was observed over a 1-h period. Several samples prepared and treated in this manner were analyzed by x-ray diffraction, which showed a structureless background with a very slight, less than 5%, contribution from crystalline regions with (111) planes oriented parallel to the sample surface. Scanning electron microscopy also showed a very poorly defined structure with small granular particles.

The spectra were recorded on the University of Illinois beamline at the Synchrotron Radiation Center, Stoughton, WI. This beamline is equipped with an ultrahigh-vacuum-analysis chamber containing a hemispherical energy analyzer, which can be rotated in both the horizontal and vertical planes.³⁸ The radiation from the Aladdin storage ring was monochromated by an extended-range grasshopper (ERG) monochromator.³⁹ The total instrumental resolution, as determined by the sharpness of the Fermi edge of metallic silver, ranged from about 0.2 eV at photon energies of 60 eV to about 0.95 eV at 165 eV.

III. RESULTS AND DISCUSSION

Typical sets of EDC's for AgBr and $\text{AgBr}_{1-x}\text{I}_x$ are shown in Fig. 1. The inelastic background was approximated by a polynomial fit to the low- and high-binding-energy sides of the valence-band features. This background was then removed and the EDC's normalized to a constant integrated area. The binding energies were measured relative to the valence-band maximum, which was determined by extrapolating the leading edge to the baseline. Because of the unusually slow rise of the band edge, the uncertainty in this determination can be as large as 0.2 eV, particularly at high photon energies near the Ag

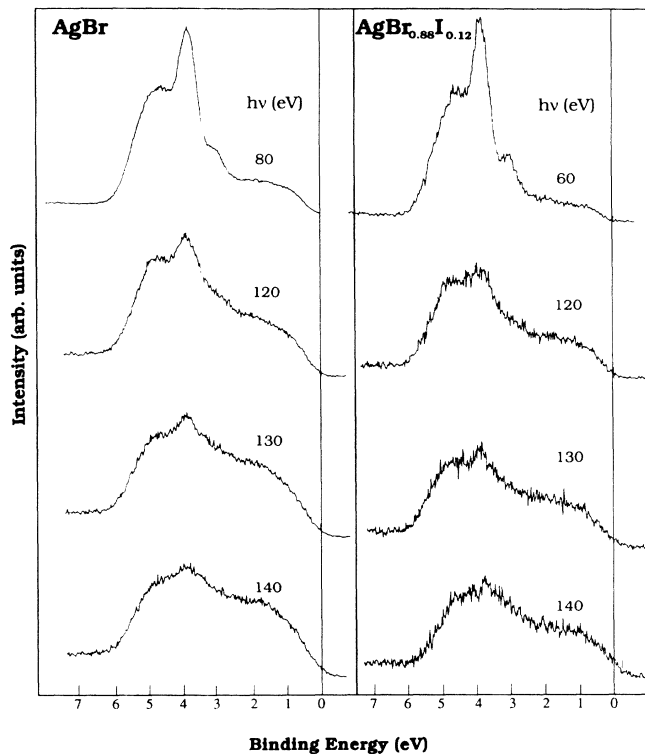


FIG. 1. Energy-distribution curves for the valence bands of silver bromide and silver iodobromide below and through the Cooper minimum. The binding energy has been referenced to the top of the valence band, with corrections made for instrumental resolution.

4*d* Cooper minimum. The effects of this minimum are clearly observable at about 130 eV.

At photon energies from about 50 to 90 eV the Ag 4*d* cross section is more than 10 times that of the bromide 4*p* (iodide 5*p*) valence levels.²⁴ In this energy region the experimental spectra give a fairly accurate representation of

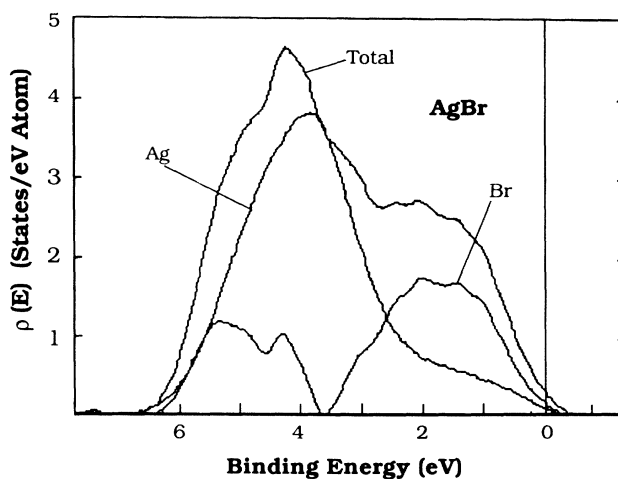


FIG. 2. Experimentally determined partial and total density of states for silver bromide determined from EDC's at 90 and 165 eV. Note the almost total absence of bromide contribution near the center of the band.

the pure silver density of states. As the Cooper minimum is approached, the spectral shape changes dramatically. The silver ionization cross section drops precipitously and the energy resolution becomes poorer. At the minimum, the halogen and silver valence cross sections are much more equal and the EDC's more representative of a true, total density of states broadened in energy. The substantial increase in relative intensity near the top of the valence band is due to the enhanced halide contribution as the silver cross section declines. In going to yet

higher photon energies, the silver cross section increases slightly and then falls off very slowly while those of the halogens continues their gradual decrease at values less than that of the silver. At no time, even very near threshold, is the halogen cross section expected to be large enough to give an EDC indicative of the pure halogen density of states.⁴⁰

To determine the halogen, and hence the total density of states, Eq. (1) must be solved for $\rho_d(E)$ and $\rho_p(E)$:

$$\rho_d = \frac{N(E, h\nu_1)C(h\nu_2)\sigma_p(h\nu_2) - N(E, h\nu_2)C(h\nu_1)\sigma_p(h\nu_1)}{C(h\nu_1)C(h\nu_2)[\sigma_d(h\nu_1)\sigma_p(h\nu_2) - \sigma_d(h\nu_2)\sigma_p(h\nu_1)]} \quad (5a)$$

and

$$\rho_p = \frac{N(E, h\nu_1)C(h\nu_2)\sigma_d(h\nu_2) - N(E, h\nu_2)C(h\nu_1)\sigma_d(h\nu_1)}{C(h\nu_1)C(h\nu_2)[\sigma_d(h\nu_2)\sigma_p(h\nu_1) - \sigma_d(h\nu_1)\sigma_p(h\nu_2)]} \quad (5b)$$

The ionization cross sections were taken from the tabulation of Yeh and Lindau,²⁴ with corrections made for ionic orbital occupations. No further adjustments were made for the ionic nature of the materials. However, the Ag 4d values were modified by a 10-eV shift in photon energy to account for the discrepancy between the calculated and experimental energies of the Cooper minimum: 120 and 130 eV,^{24,23} respectively. The partial densities of states, Eq. (5), were then solved simultaneously, at each data point, for pairs of EDC's, $N(E, h\nu)$. Since the solutions to Eq. (5) are essentially normalized difference spectra, it is imperative that the EDC pairs used as input data have nearly identical energy resolution. This was accomplished by computer broadening to produce a resolution-matched pair. The total instrumental resolution, monochromator plus energy analyzer, was determined for all relevant photon energies from the experimentally measured broadening of the Fermi level in metallic silver.

In principle, there is considerable redundancy in these experiments since a large number of spectra were recorded at photon energies from 55 to 165 eV. Halogen and silver partial densities of states can be generated from any pair of these EDC's recorded at different photon energies. In practice, three criteria were used to choose pairs for the most credible results: (1) The two photon energies should be such that there is a significant difference in the cross sections $\sigma_i(h\nu)$ and $\sigma_i(h\nu')$; (2) one of these photon energies should be in the range where the Ag 4d cross section is clearly dominant, and (3) the second photon energy should be in a region where there are no rapid changes in either the silver or halogen cross section. These criteria virtually dictate that the spectral pairs be chosen from opposite sides of the Cooper minimum. Figure 3 shows the experimentally derived AgBr partial and total densities of states which have been calculated from EDC's recorded at $h\nu=90$ and 165 eV. The general form of the PDOS is independent of the chosen EDC's. The largest changes were observed in the halogen density, with some variation in the depth of the minimum and the distribution of intensity between the low- and high-

binding-energy bands. However, a near-zero minimum is always observed between the two bands as is the structure on the high-binding-energy band near 4.5 eV.

The effects of broadening to match resolutions can be clearly seen by comparing the silver partial density of states in Fig. 2 to the $h\nu=80$ eV EDC in Fig. 1. The 80-

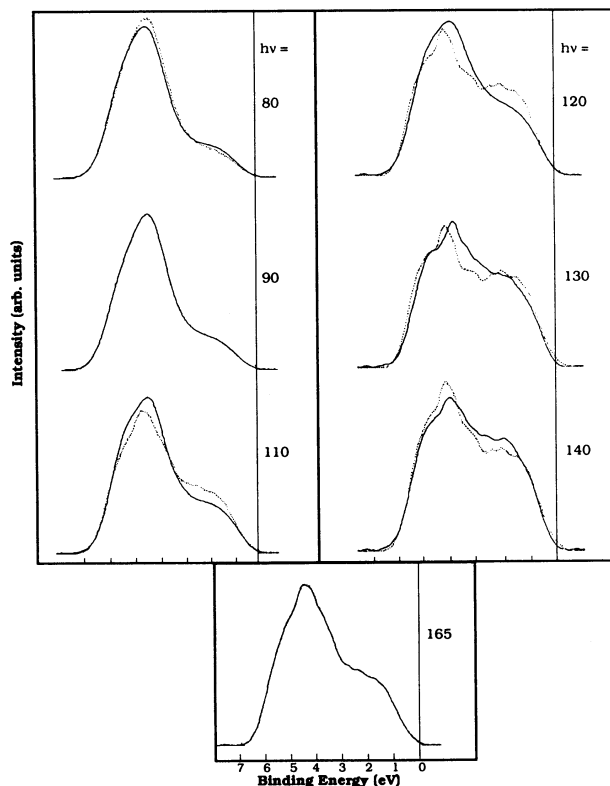


FIG. 3. The solid lines are experimentally measured energy-distribution curves. The dotted curves are determined from Eq. (1) using the PDOS in Fig. 3 and the theoretical photoionization cross sections from Ref. 24.

eV spectrum should, in itself, give a very accurate representation of the true silver DOS. This is equally true of any EDC recorded in the 50–90-eV range. The 90-eV EDC has been used because it requires less broadening to match resolution and the background subtraction is simpler. Unfortunately, it must still be broadened considerably in order to determine the halogen counterpart. This limitation is inherent in the accessible photon energy range of these measurements. The silver PDOS can always be determined with greater resolution than is possible for the halogen. Fortunately, theoretical calculations to be presented below show no sharp structural features, which might be obscured by this broadening.

The greatest limitation to this method is clearly the absence of absolute ionization cross sections. These are not known experimentally for any of the elements of interest here. Those of chlorine have been measured out to 78.5 eV,³⁴ and are about 25% larger than the calculated values from Ref. 24. If anything, the theory should be better at higher energies away from threshold and the Cooper minimum. Calculated values for bromine are expected to have a similar degree of error. On the other hand, theoretical values for the neighboring rare gases reproduce experimental measurements fairly well for both chlorine and bromine.^{32,33}

The cross sections for silver are perhaps somewhat more questionable. The total absolute ionization cross section for silver has been measured, but not the individual orbital contributions required for the PDOS determinations.⁴¹ Comparison of the calculated and experimental total cross sections for photon energies above 130 eV agree within 10%, lending credence to the theoretical values. Below 130 eV and above 300 eV the agreement is much poorer because of problems associated with the Cooper minimum on the low-photon-energy side and the 3*d* threshold on the high-photon-energy side. Fortunately, the uncertainties at low photon energy are not a serious limitation. It is simply sufficient that the Ag 4*d* cross section be much larger than that of the halogen.

One way to observe the effects of possible errors in this procedure is to compare PDOS calculations for all possible pairs of EDC's. If the approximations in Eq. (5) are correct and the cross sections are accurately known, then all of the PDOS will be identical except for differences in resolution. The degree to which variations do occur will give a good measure of the cross-section inaccuracies. This is computationally laborious and produces such a large number of PDOS curves that comparisons are difficult. A more concise method has been used by Wright *et al.* in their study of Cu-Pd alloys.²⁶ If the PDOS, which have been determined from EDC's at any two photon energies, are correct, and if the calculated cross sections are correct, then the EDC's at all other photon energies can be calculated from Eq. (1). The comparison between experimental EDC's and those calculated in this manner are shown in Fig. 3. The PDOS used in these calculations were those in Fig. 2, which were determined from EDC's at 90 and 165 eV. In general, the agreement is fair at best with significant variations in both peak positions and intensities. The deviations are the greatest in the neighborhood of the Cooper

minimum, around 120–130 eV. This is the photon-energy range where the Ag 4*d* ionization is no longer dominant and experimental and theoretical total cross sections show significant differences.

In order to assess the effects of uncertainties in σ on the PDOS determination, we have repeated the calculations using cross sections based as closely as possible on the limited experimental results available. To do this, the Ag 4*d* relative cross sections reported earlier²³ were normalized to the absolute measurements of Hagemann *et al.* at 55 eV.⁴⁰ This is the lowest accessible photon energy and is just below the Ag 4*p* threshold. At this energy the 4*d* cross section is accurately approximated by the total cross section (the only other contribution, the Ag 5*s*, is negligible²⁴). These normalized values give a silver PDOS that is imperceptibly different from that reported above (see Fig. 2). The comparison is not so good for the bromide. In Fig. 4 the bromide density of states is compared to that obtained previously using both cross sections from Yeh and Lindau.²⁴ There is a significant decrease in the intensity of the high-binding-energy component of the bromide density with the overall shape remaining fundamentally the same. This variation is probably indicative of the total quantitative uncertainty in the determination of the halogen PDOS. While other factors^{9,26} may contribute to this error, the lack of reliable cross-section data is no doubt the most serious shortcoming.

The AgBr results in Fig. 2 are generally in good agreement with those of Tejada *et al.*¹⁰ obtained at room temperature using rare-gas resonance lines. Even though the experimental resolution should have been higher in this previous work, we clearly observe greater structural detail in the present study. This is most likely due to the instability of the silver halides at room temperatures. They decompose readily at such temperatures when exposed to greater than band-gap-energy radiation. Over a period of approximately 1 h of room-temperature exposure, the Br

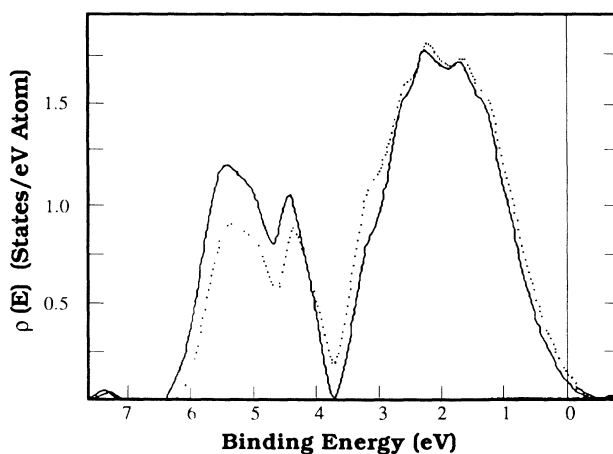


FIG. 4. Partial bromide density of states for AgBr. The solid curves were determined from the theoretical cross sections of Ref. 24 and the dotted curves are determined using the normalized relative cross sections of silver metal (see text).

3d intensity dropped by 26% due to photolysis. Most, if not all, of this loss occurred in the first stages of exposure. This should produce EDC's with contributions from both the silver halide and the photoinduced, small silver clusters. The silver halides are also known to show a "giant temperature effect" in photoemission,²⁷⁻²⁹ with intensities and peak widths changing drastically between room and liquid-nitrogen temperatures. Some of these effects are illustrated in Fig. 5, which shows the temperature dependence of EDC's recorded at 90 and 140 eV. Given these significant changes in the EDC's with temperature, it may seem surprising that the PDOS of the two studies agree as well as they do. This is probably due to the near degeneracy of the Ag 4d states in silver clusters and in the halides.

Clearly measurements on silver halides, which require exposure to high-intensity radiation, should be carried out at low temperature whenever possible. Below about 130 K the ionic mobility of AgBr is effectively quenched³⁰ and no photolysis is discernible in the Br 3d intensity. In view of this and the significant line narrowing that occurs as the temperature is lowered, most of the EDC's in this study were recorded at liquid-nitrogen temperature. Room-temperature measurements were made only for the purpose of comparison with the earlier studies.

Finally, we compare our experimental AgBr PDOS with the results of band theory. The electronic structure was calculated using the nonrelativistic, self-consistent Hartree-Fock method discussed in Ref. 15. The projected *p* and *d* densities were determined and are superimposed on the experimental PDOS in Fig. 6. To account

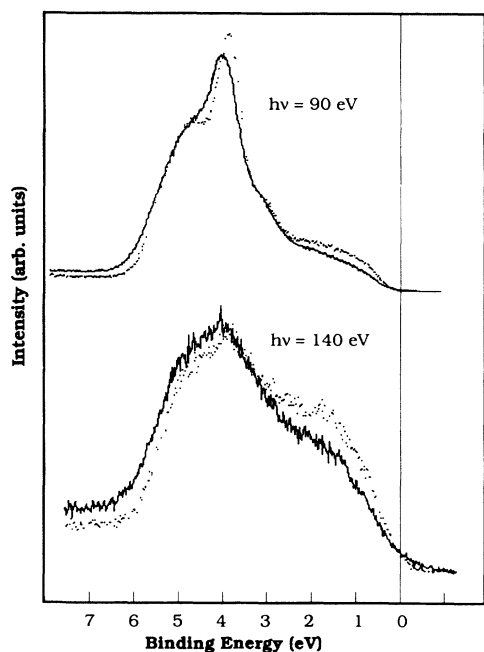


FIG. 5. Energy-distribution curves for silver bromide recorded at 77 K (dotted lines) and room temperature (solid lines). These changes persist when the room-temperature-exposed sample is recooled to 77 K.

for the experimental resolution the calculated curves have been convoluted with a 0.95-eV, full width at half maximum (FWHM), Gaussian line shape. This width was determined from broadening of the Fermi level of metallic silver. No attempt has been made to account for the lifetime broadening of unknown value. The qualitative shapes of the PDOS are very well described by theory. Quantitatively, however, the position of the sharp peak in the silver density is too tightly bound relative to the valence-band maximum. This causes the calculated density to be slightly too broad. Also, the theoretical density in the neighborhood of the band maximum is too large. This latter problem is prevalent in several other, much less sophisticated, semiempirical, calculations for AgCl.¹⁰⁻¹² As pointed out in Ref. 10, the valence-band maximum is associated with a region of high state density at the edge of the Brillouin zone. This would normally produce a much sharper edge than is seen experimentally. Significant sharpening is observed as the temperature is lowered from 300 to 77 K. Recent extended x-ray-absorption fine-structure (EXAFS) studies⁴² show that substantial vibrational effects persist in AgBr down to 20 K. It seems reasonable to suggest that the apparent, low state density near the band maximum results from the unusual thermal-broadening effects in these materials.²⁷⁻²⁹

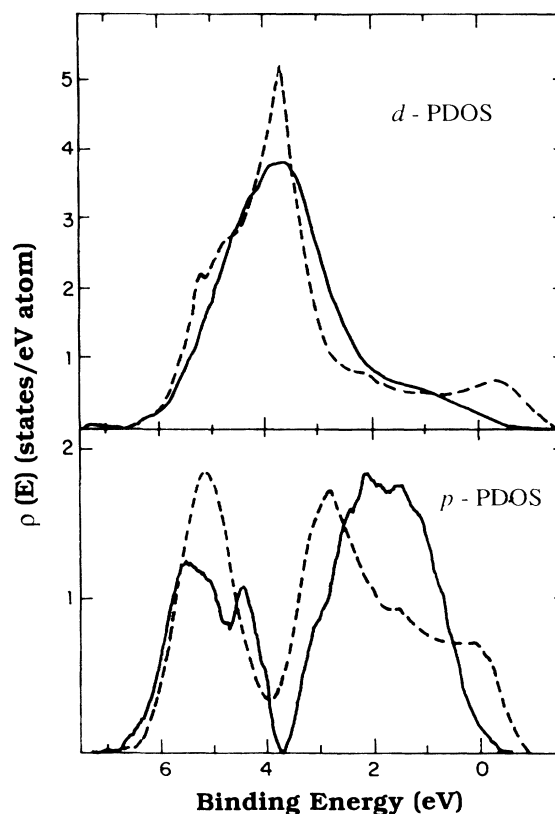


FIG. 6. Comparison of experimental (solid curves) and theoretical (dashed curves) partial *p* and *d* DOS's for AgBr. Theoretical curves have been convoluted with a 0.95-eV, FWHM Gaussian to simulate the effects of experimental resolution and the binding-energy zero has been arbitrarily set.

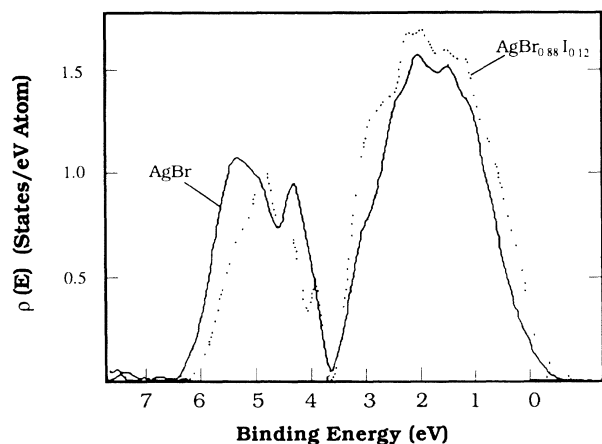


FIG. 7. Halogen partial density of states for AgBr and AgBr_{0.88}I_{0.12}. Note the broadening of the low-binding-energy component with iodide inclusion and the upward movement of the valence-band maximum. Also note the scale change between the *p* and *d* densities of states.

The effect of iodide addition to AgBr is shown in Fig. 7 (see also Fig. 1). The iodide concentration was estimated to be about 12% based on the intensity of the I 4*d* and Br 3*d* emissions at 100 eV photon energy. Here the uncertainty is large because both cross sections are changing very rapidly with photon energy. There is also a possibility of phase separation in this sample, but no indication of a pure iodide can be seen in any of the EDC's and the core lines are all sharp and symmetrical, as would be expected for a single component. Notice that the silver PDOS is only slightly modified relative to the pure bromide, but some interesting changes are seen in the halogen PDOS.

Because the Br 4*p* and I 5*p* cross sections are very similar throughout the accessible photon-energy range, we are unable to separate the halogen PDOS into its constituent contributions. In Fig. 7 the total halogen density of states in the iodobromide is compared to that of pure

silver bromide. The absence of a clear reference point makes a quantitative comparison difficult. On the basis of previous x-ray-photoemission (XPS) results, we have assumed that the position of the sharp atomiclike structure, which produces the minimum at about 4 eV binding energy, is a reasonable reference energy.⁴³ Within this assumption, the topmost portion of the halogen density moves upwards towards the vacuum level with iodide addition. This is consistent with the change in band gap, which narrows by 0.2 eV in a 12 mol % iodide,⁴⁴ and with XPS studies that show that the entire narrowing of the band gap is due to the upward motion of the valence band.⁴³ The small steplike feature at the very top of the iodobromide PDOS may not be real and is possibly due to errors in the background subtraction. A similar feature has, however, been seen in XPS spectra of iodobromide crystals.⁴³

Independent of this assumption, the low-binding-energy peak increases in intensity and broadens, while the high-binding-energy component does just the opposite. This is entirely consistent with the expectations of simple molecular-orbital theory. The ionization potential of an iodide is about 0.3 eV less than that of a bromide.⁴⁵ This should cause both the bonding and antibonding orbitals to move to lower binding energy, with the greatest effect taking place in the antibonding states near the top of the valence band.

ACKNOWLEDGMENTS

The authors would like to thank T. Schauman for his help in sample preparation. We would also like to acknowledge support from the U.S. National Science Foundation (NSF) under Grant No. DMR-88-96157 and from the U.S. Navy (Office of Naval Research) under Grant No. ONR-N0014-89-J-1. Additional support from Eastman Kodak Company (Rochester, NY) is also much appreciated. The Synchrotron Radiation Center (Stoughton, WI) is supported by the NSF under Grant No. DMR-86-01349.

*Present address: A. G. Edwards and Sons, St. Louis, Missouri 63131.

¹L. J. Page and E. H. Hugh, *Phys. Rev. B* **1**, 3472 (1970).

²P. H. Citrin and T. D. Thomas, *J. Chem. Phys.* **57**, 4446 (1972).

³F. Seitz, *Modern Theory of Solids* (McGraw-Hill, New York, 1940).

⁴R. S. Knox, F. Bassani, and W. B. Fowler, *Photographic Sensitivity* (Maruzen, Tokyo, 1963), Vol. III, p. 11.

⁵F. Bassani, R. S. Knox, and W. B. Fowler, *Phys. Rev.* **137**, A1217 (1965).

⁶P. M. Scop, Massachusetts Institute of Technology Solid State and Molecular Theory Group, Quarterly Progress Report No. 54, Oct. 1964 (unpublished); *Phys. Rev.* **139**, A934 (1965).

⁷W. B. Fowler, *Phys. Status Solidi B* **52**, 591 (1972).

⁸R. C. Birtcher, P. W. Deutsch, T. F. Wendelken, and A. B. Kunz, *J. Phys. C* **5**, 562 (1972).

⁹A. Goldmann, J. Tejada, N. J. Shevchik, and M. Cardona,

Phys. Rev. B **10**, 4388 (1974).

¹⁰J. Tejada, N. J. Shevchik, W. Braun, A. Goldmann, and M. Cardona, *Phys. Rev. B* **12**, 1557 (1975).

¹¹J. S.-Y. Wang, M. Schlüter, and M. L. Cohen, *Phys. Status Solidi B* **77**, 295 (1976).

¹²P. V. Smith, *J. Phys. Chem. Solids* **37**, 581 (1976); **37**, 589 (1976).

¹³H. Overhof, *J. Phys. Chem. Solids* **38**, 1214 (1977).

¹⁴S. Ves, D. Glotzel, M. Cardona, and M. Overhof, *Phys. Rev. B* **24**, 3073 (1981).

¹⁵A. B. Kunz, *Phys. Rev. B* **26**, (1982).

¹⁶W. von der Osten, in *The Physics of Latent Image Formation in Silver Halides*, edited by A. Baldereschi, W. Czaja, E. Tosatti, and M. Tosi (Taylor and Francis, Philadelphia, 1984).

¹⁷M. G. Mason, *J. Electron Spectrosc. Relat. Phenom.* **5**, 573 (1974).

¹⁸M. G. Mason, *Phys. Rev. B* **11**, 5094 (1975).

- ¹⁹G. K. Wertheim, Phys. Rev. B **36**, 4432 (1987).
- ²⁰P. S. Wehner, J. Stohr, G. Apai, F. R. McFeely, R. S. Williams, and D. A. Shirley, Phys. Rev. B **14**, 2411 (1976).
- ²¹M. O. Krause, W. A. Svensson, T. A. Carlson, G. Leroi, D. E. Ederer, D. M. P. Holland, and A. C. Parr, J. Phys. B **18**, 4069 (1985).
- ²²M. Ardehali and I. Lindau, J. Electron Spectrosc. Relat. Phenom. **46**, 215 (1988).
- ²³G. N. Kwawer, T. J. Miller, M. G. Mason, Y. Tan, F. C. Brown, and Y. Ma, Phys. Rev. B **39**, 1471 (1989); G. N. Kwawer, Ph.D. thesis, University of Illinois, 1989.
- ²⁴J. J. Yeh and I. Lindau, At. Data Nucl. Data Tables **32**, 1 (1985).
- ²⁵W. Braun, A. Goldmann, and M. Cardona, Phys. Rev. B **10**, 5069 (1974).
- ²⁶H. Wright, P. Weightman, P. T. Andrews, W. Folkerts, C. F. J. Flipse, G. A. Sawatzky, D. Norman, and H. Padmore, Phys. Rev. B **35**, 519 (1987).
- ²⁷R. S. Bauer, S. F. Lin, and W. E. Spicer, Phys. Rev. B **14**, 4527 (1976).
- ²⁸R. S. Bauer and W. E. Spicer, Phys. Rev. B **14**, 4539 (1976).
- ²⁹R. S. Bauer, Ph.D. thesis, Stanford University, 1970 (University Microfilms No. 71-19646).
- ³⁰R. S. Eachus, R. E. Graves, and M. T. Olm, J. Chem. Phys. **69**, 4580 (1978); R. S. Eachus and R. E. Graves, *ibid.* **65**, 1530 (1976); R. S. Eachus (unpublished).
- ³¹P. C. Kemeny, R. T. Poole, J. G. Jenkin, J. Liesegang, and R. C. G. Leckey, Phys. Rev. A **10**, 190 (1974).
- ³²D. J. Kennedy and S. T. Manson, Phys. Rev. A **5**, 227 (1972).
- ³³J. A. R. Samson, Adv. At. Mol. Phys. **2**, 178 (1976).
- ³⁴J. A. R. Samson, Phys. Rev. Lett. **56**, 2020 (1986).
- ³⁵R. Courths and S. Hüfner, Phys. Rep. **112**, 53 (1984), and references therein.
- ³⁶Contrary to the claims of Ref. 10, we found that the best films were formed by slow, low-temperature evaporations. This was confirmed by core-level studies from the evaporated films and bulk crystals.
- ³⁷R. C. Baetzold, Y. T. Tan, and P. W. Taskor, Surf. Sci. **195**, 579 (1986).
- ³⁸T. J. Miller, Ph.D. thesis, University of Illinois, 1986.
- ³⁹S. L. Hulbert, J. P. Stott, and F. C. Brown, Nucl. Instrum. Methods Phys. Res. **208**, 43 (1983).
- ⁴⁰The cross sections of Ref. 24 would predict that Ne I radiation (16.8 eV) would give primarily a halogen PDOS. However, the experimental results of Ref. 10 show that a strong silver contribution is present.
- ⁴¹H. J. Hagemann, W. Gudat, and C. Kunz, J. Opt. Soc. Am. **65**, 742 (1975).
- ⁴²Y. T. Tan (unpublished).
- ⁴³M. G. Mason (unpublished).
- ⁴⁴A. P. Marchetti and M. Burberry, Phys. Rev. B **37**, 10862 (1988).
- ⁴⁵H. Hotop and W. C. Lineberger, J. Phys. Chem. Ref. Data **14**, 731 (1985).